

**COMBINED METHOD OF THE RAILWAY BRIDGES DYNAMIC
RESPONSE COMPUTATION ADAPTED TO DEVELOPING
COUNTRIES: THE CASE OF THE SECOND BRIDGE OVER THE
WOURI IN CAMEROON**

**Ursula Joyce Merveilles Pettang Nana*^{1a}, Cedric Cabral Fandjio Yonzou^b and
Marcelline Manjia^c**

^aPhD Doctor, Department of Civil Engineering, National Advanced School of Engineering,
University of Yaounde I, P.O. Box 8390, Yaoundé, Cameroon.

^bIngénieur de Conception, Department of Civil Engineering, National Advanced School of
Engineering, University of Yaounde I, P.O. Box 8390, Yaoundé, Cameroon.

^cMaître de Conférence, Department of Civil Engineering, National Advanced School of
Engineering, University of Yaounde I, P.O. Box 8390, Yaoundé, Cameroon.

Article Received on 22/06/2021

Article Revised on 12/07/2021

Article Accepted on 02/08/2021

***Corresponding Author**

**Ursula Joyce Merveilles
Pettang Nana**

PhD Doctor, Department of
Civil Engineering, National
Advanced School of
Engineering, University of
Yaounde I, P.O. Box 8390,
Yaoundé, Cameroon.

SUMMARY

The modernisation of the railway sector, in particular through the introduction of new, high-performance rolling stock, as required by the UA65 strategy, implies taking into account the particularly formidable dynamic loads on existing bridges. In order to make this equipment useful and to integrate it into the development of the railway network, which is now desired to be of a high standard, a prior diagnostic analysis makes it possible to classify which of these structures should be preserved or renovated. With this in mind, this paper presents a

simplified combined method for calculating the dynamic response of railway bridges in order to simulate their behaviour in service. Using the Finite Element Method (FEM), we worked with a three-layer unequal element track model and a 10 degree of freedom vehicle model. The main excitation of the system is the set of irregularities of the track taken into account by the sinusoidal PSD function of the German model. The interaction forces were expressed using the linear Kalker theory. The resulting 2D matrix equation of motion of the train was

solved by Newmark's β numerical method. The simulation carried out on the second bridge over the Wouri river, allowed on the one hand to verify the proposed method with convincing results which present limits at the level of the continuity of the railway track on firm ground (when the train is not entirely on the bridge) and on the other hand to note that existing bridges such as the Wouri river are able to receive locomotives at higher speeds (220km/h) without significant modification of the structure.

KEYWORDS: Dynamic loads, rail bridges, FEM, Newmark's β method.

INTRODUCTION

The flow of goods and people in Africa has been increasing significantly according to IMF data since 2013. This growth absolutely requires a quality rail transport sector, because as elsewhere in the world the rail sector has many assets that catalyse economic growth [Michel Leboeuf, 2016]. However, rail traffic is stagnating in Africa while it has been growing exponentially since the 2000s worldwide. Indeed, apart from South Africa, the rail network in sub-Saharan Africa is fragmented and not very coherent [Pourtier R., 2007]. Compared to colonial times, it remains very small and in very poor condition [Olievschi V. N., 2013]. In addition, there is a shortage of railway expertise at all levels of the sector [ADB, 2015]. This lack of knowledge inevitably undermines the prospects for modernising the railway fleet and infrastructure, which is a matter of mastering dynamic train-bridge analysis. It has often been sufficient to take into account the dynamic effects by means of a so-called *dynamic amplification* coefficient, which is no longer sufficient today. On the one hand because most modern trains (even freight trains) exceed 80 km/h (SNCF standards), and on the other hand because this approach does not take into account all the phenomena generating dynamic effects, as well as resonance effects [EC1-2, 2004].

Dynamic railway analysis is more than 180 years old and has become a very topical area due to the technological evolution of the sector. Despite the large amount of work on the subject, it still has a complex character due to the multiple factors related to the train and the railway track [Zhang N. *et al.* , 2016]. In fact, the nodes of difficulty that we will address lie not only in the accuracy of the models representing the vehicle/bridge systems, but also in the interaction between them. After the presentation of the mechanical model of train-track-bridge system and the dynamic nature of the {vehicle/track} system, we propose a combined calculation method adapted to the growing of developing countries. The application of this method to the second bridge over the Wouri in Cameroon allows to conclude on its relevance.

Mechanical model of the train-track-bridge system

Modelling choices for the track-bridge sub-system

In order to focus on the forces transmitted on the bridge deck, the bridge bearings, piers and foundations can be dissociated from the model [Kourousis G., 2009]. Recent work shows that the most relevant models for characterising each essential component of the track model are listed below.

- The bridge deck: it is discretised into "bridge" elements each modelled by a Euler-Bernoulli beam of length l_{be} , strictly greater than the length of the rail element $l_{\mathfrak{R}}$ in order to speed up the numerical processing [Lou P. *et al.*, 2012].
- The rail: the model used for each rail element is also the Euler-Bernoulli beam. It is a simplistic model which remains valid when only vertical motion is considered and with vibrations below 500Hz [Kourousis G., 2009].
- The sleepers: they are taken into account in the most accurate track models [Lou P. *et al.*, 2012], each represented by a rigid rod of concentrated mass m_s . They are spaced from each other by a length l_{sp} .
- The attachment systems (or footings) and ballast: their vertical elasticity and damping properties are modelled as springs and massless dampers represented by a stiffness k_{rs} and a damper c_{rs} on the one hand; and a series of spring k_{sb} and a damper c_{sb} .

The whole set is connected as seen in the diagram below. It is assumed for convenience that the length l_{be} equals a multiple of the length $l_{\mathfrak{R}}$. The rail and bridge elements are Euler-Bernoulli beams whose properties are Young's modulus E_r , E_b modulus; quadratic moduli I_r , I_b ; cross sections A_r , A_b and linear masses ρ_r , ρ_b where the subscripts r and b denote the rail and the bridge respectively.

The illustration of these elements of the unequal element bridge-rail coupling model is shown in figure 1.

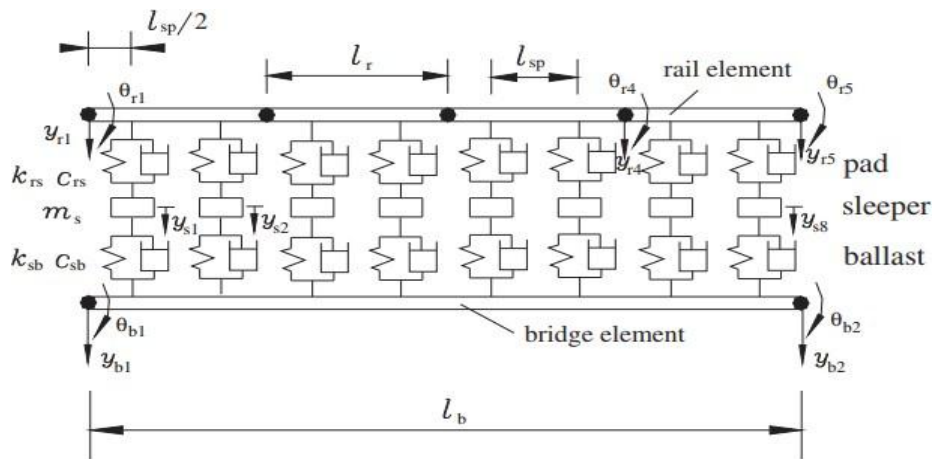


Figure 1: A rail-bridge coupling element of unequal lengths [Lou P. et al., 2012].

1.1 Modelling choices for the train subsystem

The train is composed of several elements running at the same speed called vehicles (the wagons and the locomotive), which are assumed to be disjoint and independent [Zhang N. et al., 2010] as they are N_v on a given track. In order to take into account the characteristics of the train, we introduce the vehicle as a multi-body system (the different vehicle models being explained in [Kourousis G. et al., 2014]). We choose the 2D model, described by [Cantero D., 2015], which also offers results close to those of the 3D model (less than 1% difference for vertical displacements [Zeng Z.-P. et al. , 2016]). Each vehicle will have 10 ddl, the seven vertical displacements of the masses (wheel, bogie and body) and the three rotations of the rigidbars (bogie and body). An example of vehicle model is given in figure 2.

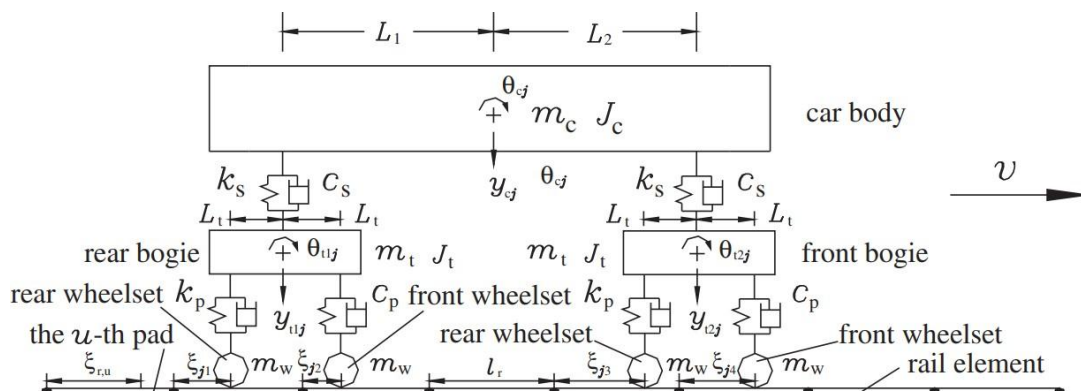


Figure 2: Vehicle model with its ddl [Lou P., 2012].

Dynamic nature of the {vehicle/track} system

The source of excitement

The main source of excitation of the track is all its irregularities. We will use the power spectral density function PSD of the German model, which includes all the types of

irregularities found on old African railways. It is defined by the following equation where $\Omega_r = 0.0206 \text{ rad/m}$; $\Omega_c = 0.8246 \text{ rad/m}$. The degree of roughness A_V of the track is defined by a range of values from $A_V = 4.032 \times 10^{-7} \text{ m}^2/(\text{rad/m})$ for tracks in good condition to $A_V = 10.80 \times 10^{-7} \text{ m}^2/(\text{rad/m})$ for tracks in poor condition.

Longitudinal levelling defect: $S^V(\Omega) = \frac{A_V \Omega_c^2}{(\Omega^2 + \Omega_r^2)(\Omega^2 + \Omega_c^2)} \tag{1}$

Misalignment : $S^A(\Omega) = \frac{A_A \Omega_c^2}{(\Omega^2 + \Omega_r^2)(\Omega^2 + \Omega_c^2)} \tag{2}$

Level defect: $S^C(\Omega) = \frac{(A_V/b_0^2)\Omega_c^2 \Omega^2}{(\Omega^2 + \Omega_r^2)(\Omega^2 + \Omega_c^2)(\Omega^2 + \Omega_s^2)} \tag{3}$

Gap between rails: $S^G(\Omega) = \frac{A_G \Omega_c^2 \Omega^2}{(\Omega^2 + \Omega_r^2)(\Omega^2 + \Omega_c^2)(\Omega^2 + \Omega_s^2)} \tag{4}$

In the case of ballasted railways, these levelling faults are largely created by the settlement of the ballast layer which directly receives the loads due to traffic [Quezada J. C., 2012].

3.2 Wheel/rail contact forces: Kalker's linear theory

Subjected to the mass of the vehicle, the steel constituting the rails and wheels deforms due to its elasticity, and the contact between them becomes surface where some points may slip, while others may roll as the two bodies move relative to each other (it's illustrated in figure 3). The small apparent slip that arises generates tangential pseudo-slip forces [Moncef Toumi, 2016] and rotational momentum [Khaled E. and Schwab A., 2009].

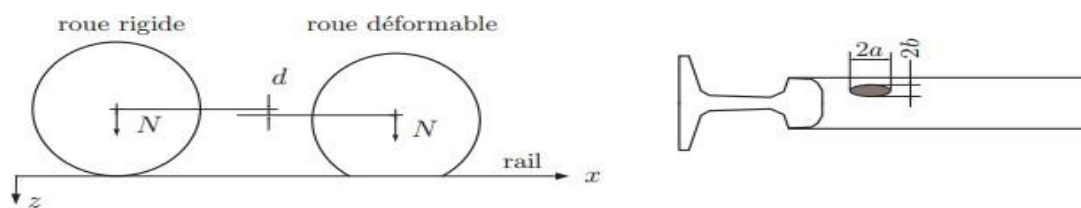


Figure 3: Herz problem applied to the railway case [Kourousis G., 2009].

$$\begin{Bmatrix} F_x \\ F_y \\ M_\varphi \end{Bmatrix} = -Gab \begin{bmatrix} C_{11} & 0 & 0 \\ 0 & C_{22} & \sqrt{ab}C_{33} \\ 0 & -\sqrt{ab}C_{33} & abC_{33} \end{bmatrix} \begin{Bmatrix} \xi_x \\ \xi_y \\ \xi_\varphi \end{Bmatrix}, \tag{5}$$

G being the shear modulus, the longitudinal, transverse and transverse pseudo-shear forces F_x and transverse F_y and the moment M_φ about the vertical axis to the longitudinal and transverse pseudo-shear components ξ_x and transverse ξ_y (f^{22} ou f_{22}) and in the vertical direction ξ_φ .

There is a complete or exact theory for the expression of pseudogloss, but the implementation is very constraining. Some authors use a simplified Kalker formulation which has a low computational cost and a satisfactory accuracy (80% to 90%).

$$\begin{Bmatrix} F_x \\ F_y \end{Bmatrix} = \begin{bmatrix} -\frac{8a^2b}{3L_x} \xi_x \\ -\frac{8a^2b}{3L_y} \xi_y - \frac{\pi a^3b}{4L_y} \xi_\varphi \end{bmatrix}, \text{ où : } \begin{cases} L_x = \frac{8a}{3C_{11}G} \\ L_y = \frac{8a}{3C_{22}G} \\ L_\varphi = \frac{\pi a^2}{4G\sqrt{ab}C_{23}} \end{cases} \quad (6)$$

Combined calculation method: Coupling and interaction equations of the vehicle/rail/bridge system.

Formulation of elasticity and damping of fasteners and ballast

In order to formulate the elasticity and damping of the fasteners and ballast, let us first consider an i-th rail element connected to a tie by a fastener as shown in Figure 3. The upper connection point of the fastener has a ddl depending on the rail movement expressed by its fourddl $(y_{r,i}; \theta_{zr,i})$ and $(y_{r,i+1}; \theta_{zr,i+1})$ while the lower connection point has a ddl dependent on the vertical movement y_s of the sleeper.

The elastic deformation energy of a discrete spring of the clamp taken at the position $\xi_{rs} = x_{rs}/l_{\mathfrak{R}}$ is written as:

$$\begin{aligned} \varepsilon_{pad}^{y,e} &= \frac{1}{2} k_{rs} (N_{r,1}y_{r,i} + N_{r,2}\theta_{zr,i} + N_{r,3}y_{r,i+1} + N_{r,4}\theta_{zr,i+1} - y_s)^2 \\ &= \frac{1}{2} k_{rs} \begin{bmatrix} y_{r,i} \\ \theta_{zr,i} \\ y_{r,i+1} \\ \theta_{zr,i+1} \\ y_s \end{bmatrix}^T \times \begin{bmatrix} N_{r,1}N_{r,1} & N_{r,1}N_{r,2} & N_{r,1}N_{r,3} & N_{r,1}N_{r,4} & -N_{r,1} \\ & N_{r,2}N_{r,2} & N_{r,2}N_{r,3} & N_{r,2}N_{r,4} & -N_{r,2} \\ & & N_{r,3}N_{r,3} & N_{r,3}N_{r,4} & -N_{r,3} \\ & & & N_{r,4}N_{r,4} & -N_{r,4} \\ & & & & 1 \end{bmatrix} \times \begin{bmatrix} y_{r,i} \\ \theta_{zr,i} \\ y_{r,i+1} \\ \theta_{zr,i+1} \\ y_s \end{bmatrix} \\ &= \frac{1}{2} [y_{r,i} \ \theta_{zr,i} \ y_{r,i+1} \ \theta_{zr,i+1} \ y_s] \mathbf{k}_{pad}^e [y_{r,i} \ \theta_{zr,i} \ y_{r,i+1} \ \theta_{zr,i+1} \ y_s]^T \quad (7) \end{aligned}$$

Hence the elementary elasticity matrix of a fastener :

$$\mathbf{k}_{pad}^e = k_{rs} \begin{bmatrix} N_{r,1}N_{r,1} & N_{r,1}N_{r,2} & N_{r,1}N_{r,3} & N_{r,1}N_{r,4} & -N_{r,1} \\ & N_{r,2}N_{r,2} & N_{r,2}N_{r,3} & N_{r,2}N_{r,4} & -N_{r,2} \\ & & N_{r,3}N_{r,3} & N_{r,3}N_{r,4} & -N_{r,3} \\ & & & N_{r,4}N_{r,4} & -N_{r,4} \\ & & & & 1 \end{bmatrix}_{\xi=\xi_{rs}} \quad (8)$$

With :

$$\begin{aligned} N_{1,r}(\xi_{rs}) &= 1 - 3\xi_{rs}^2 + 2\xi_{rs}^3 \\ N_2(\xi_{rs}) &= (\xi_{rs} - 2\xi_{rs}^2 + \xi_{rs}^3)l_{\mathfrak{R}} \\ N_3(\xi_{rs}) &= 3\xi_{rs}^2 - 2\xi_{rs}^3 \\ N_4(\xi_{rs}) &= (-\xi_{rs}^2 + \xi_{rs}^3)l_{\mathfrak{R}} \text{ où } \xi_{rs} = \frac{x_{rs}}{l_{\mathfrak{R}}} \end{aligned}$$

Similarly, the elementary damping matrix of a tie is also a matrix 5×5 deduced from the previous one by replacing k_{rs} by c_{rs} .

$$\mathbf{c}_{pad}^e = c_{rs} \begin{bmatrix} N_{r,1}N_{r,1} & N_{r,1}N_{r,2} & N_{r,1}N_{r,3} & N_{r,1}N_{r,4} & -N_{r,1} \\ & N_{r,2}N_{r,2} & N_{r,2}N_{r,3} & N_{r,2}N_{r,4} & -N_{r,2} \\ & & N_{r,3}N_{r,3} & N_{r,3}N_{r,4} & -N_{r,3} \\ & & & N_{r,4}N_{r,4} & -N_{r,4} \\ & & & & 1 \end{bmatrix}_{\xi=\xi_{rs}} \quad (9)$$

(sym.)

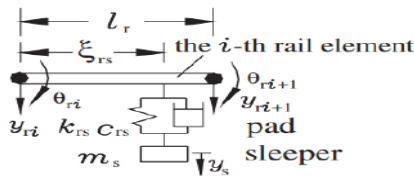


Figure 4: Connection of sleeper and ith rail element

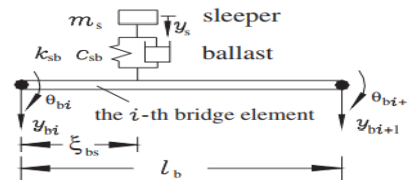


Figure 5: Connection of crossbar and ith bridge element

In a second step talking about the elasticity and damping of ballast, let us consider a sleeper connected to ani-th bridge element by ballast as shown in figure 5. The upper connection point of the ballast has a ddl depending on the vertical movement of the sleeper, while the ddl of the lower connection point is y_s of the sleeper while the ddl of the lower connection point is dependent on the motion of the bridge expressed by its four ddl $(y_{b,i}; \theta_{zb,i})$ and $(y_{b,i+1}; \theta_{zb,i+1})$. The elastic deformation energy of a discrete ballast spring taken at the position $\xi_{sb} = x_{sb}/L_{be}$ is written as:

$$\begin{aligned} \varepsilon_{ballast}^{y,e} &= \frac{1}{2} k_{sb} (y_s - N_{b,1}y_{b,i} - N_{b,2}\theta_{zb,i} - N_{b,3}y_{b,i+1} - N_{b,4}\theta_{zb,i+1})^2 \\ &= \frac{1}{2} k_{sb} \begin{bmatrix} y_s \\ y_{b,i} \\ \theta_{zb,i} \\ y_{b,i+1} \\ \theta_{zb,i+1} \end{bmatrix}^T \times \begin{bmatrix} 1 & -N_{b,1} & -N_{b,2} & -N_{b,3} & -N_{b,4} \\ & N_{b,1}N_{b,1} & N_{b,1}N_{b,2} & N_{b,1}N_{b,3} & N_{b,1}N_{b,4} \\ & & N_{b,2}N_{b,2} & N_{b,2}N_{b,3} & N_{b,2}N_{b,4} \\ & & & N_{b,3}N_{b,3} & N_{b,3}N_{b,4} \\ & & & & N_{b,4}N_{b,4} \end{bmatrix} \times \begin{bmatrix} y_s \\ y_{b,i} \\ \theta_{zb,i} \\ y_{b,i+1} \\ \theta_{zb,i+1} \end{bmatrix} \\ &= \frac{1}{2} [y_s \ y_{b,i} \ \theta_{zb,i} \ y_{b,i+1} \ \theta_{zb,i+1}] \mathbf{k}_{ballast}^e [y_s \ y_{b,i} \ \theta_{zb,i} \ y_{b,i+1} \ \theta_{zb,i+1}]^T \quad (10) \end{aligned}$$

Hence the elementary matrix of the ballast :

$$\mathbf{k}_{ballast}^e = k_{sb} \begin{bmatrix} 1 & -N_{b,1} & -N_{b,2} & -N_{b,3} & -N_{b,4} \\ & N_{b,1}N_{b,1} & N_{b,1}N_{b,2} & N_{b,1}N_{b,3} & N_{b,1}N_{b,4} \\ & & N_{b,2}N_{b,2} & N_{b,2}N_{b,3} & N_{b,2}N_{b,4} \\ & & & N_{b,3}N_{b,3} & N_{b,3}N_{b,4} \\ & & & & N_{b,4}N_{b,4} \end{bmatrix}_{\xi=\xi_{sb}} \quad (11)$$

(sym.)

$$\begin{aligned}
 N_{b,1}(\xi_{sb}) &= 1 - 3\xi_{sb}^2 + 2\xi_{sb}^3 \\
 N_{b,2}(\xi_{sb}) &= (\xi_{sb} - 2\xi_{sb}^2 + \xi_{sb}^3)l_{be} \\
 N_{b,3}(\xi_{sb}) &= 3\xi_{sb}^2 - 2\xi_{sb}^3 \\
 N_{b,4}(\xi_{sb}) &= (-\xi_{sb}^2 + \xi_{sb}^3)l_{be} \text{ où } \xi_{sb} = \frac{x_{sb}}{l_{be}}
 \end{aligned}$$

Similarly, the elementary damping matrix of the ballast is also a matrix 5×5 deduced from the previous one by replacing k_{sb} by c_{sb} .

$$\mathbf{c}_{ballast}^e = c_{sb} \begin{bmatrix} 1 & -N_{b,1} & -N_{b,2} & -N_{b,3} & -N_{b,4} \\ & N_{b,1}N_{b,1} & N_{b,1}N_{b,2} & N_{b,1}N_{b,3} & N_{b,1}N_{b,4} \\ & & N_{b,2}N_{b,2} & N_{b,2}N_{b,3} & N_{b,2}N_{b,4} \\ & & & N_{b,3}N_{b,3} & N_{b,3}N_{b,4} \\ & & & & N_{b,4}N_{b,4} \end{bmatrix}_{\xi=\xi_{sb}} \quad (12)$$

1.2 2D equations of motion of the train-track-bridge system

We will adopt an approach in generalized coordinates which allows to obtain a compact system of equations whose number is strictly equal to the number of degrees of freedom of the studied system. We only consider the case of vertical motion, so the configuration parameters taken into account are only related to vertical displacements and rotations in the plane of the paper. We take the type of model represented in figure 6 for the equations.

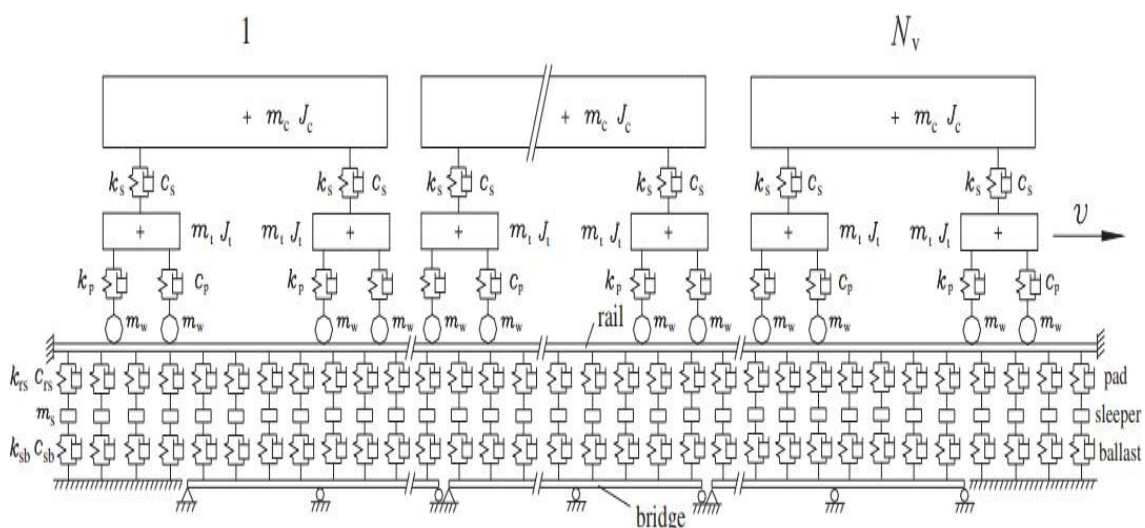


Figure 6: A typical train-track-bridge interaction system [Zeng Z.-P., 2016].

$$\begin{bmatrix} M_{vv} & 0 & 0 & 0 \\ 0 & M_{rr} & 0 & 0 \\ 0 & 0 & M_{ss} & 0 \\ 0 & 0 & 0 & M_{bb} \end{bmatrix} \begin{Bmatrix} \ddot{X}_v \\ \ddot{X}_r \\ \ddot{X}_s \\ \ddot{X}_b \end{Bmatrix} + \begin{bmatrix} C_{vv} & C_{vr} & 0 & 0 \\ C_{rv} & C_{rr} & C_{rs} & 0 \\ 0 & C_{sr} & C_{ss} & C_{sb} \\ 0 & 0 & C_{bs} & C_{bb} \end{bmatrix} \begin{Bmatrix} \dot{X}_v \\ \dot{X}_r \\ \dot{X}_s \\ \dot{X}_b \end{Bmatrix} + \begin{bmatrix} K_{vv} & K_{vr} & 0 & 0 \\ K_{rv} & K_{rr} & K_{rs} & 0 \\ 0 & K_{sr} & K_{ss} & K_{sb} \\ 0 & 0 & K_{bs} & K_{bb} \end{bmatrix} \begin{Bmatrix} X_v \\ X_r \\ X_s \\ X_b \end{Bmatrix} = \begin{Bmatrix} F_v \\ F_r \\ F_s \\ F_b \end{Bmatrix} \tag{13}$$

Where M, C and K denote the mass, damping and elasticity sub-matrices respectively, X and F represent the displacement and force vectors respectively, and the subscripts "v", "r", "s" and "b" denote the vehicle, rail, sleeper and bridge, respectively

We have written this matrix equation omitting the time parameter (t) so as not to clutter the equations.

- If N_v is the total number of vehicles,

$$X_v = [X_{v1} \ X_{v2} \ \dots \ X_{vN_v}]^T \tag{14}$$

Where X_{vj} is the vehicle displacement vectorj which is expressed as :

$$X_{vj} = [y_{cj} \ \theta_{z cj} \ y_{b1j} \ \theta_{zb1j} \ y_{b2j} \ \theta_{zb2j} \ y_{w1j} \ y_{w2j} \ y_{w3j} \ y_{w4j}] \tag{15}$$

- If N_{re} is the number of rail elements along its length, then we have $(N_{re} + 1)$ nodes.

$$X_r = [X_{r,1} \ X_{r,2} \ \dots \ X_{r,i} \ \dots \ X_{r,N_{re}+1}] \text{ with } :X_{r,i} = [y_{r,i} \ \theta_{zr,i}] \tag{16}$$

It should be noted that $l_{re} = L_{bridge}/N_{re}$ (17)

- If N_s is the total number of sleepers, $X_s = [y_{s1} \ y_{s2} \ \dots \ y_{sN_s}]^T$ (18)
- The number of bridge elements on a span can be deduced as i ($i = 1, n_{span}$), n_{be_i} by the proportionality relations :

$$n_{be_i} = \frac{L_{span_i}}{l_{be}}, \text{ tel que } \frac{l_{be}}{l_{re}} \in \mathbb{N} ; \text{ where } L_{span_i} \text{ is the length of the span } i.$$

It can be seen that an $(l_{be}; l_{re})$ ideal couple checks $L_{span} = PPMC(l_{be}; l_{re})$. Then :

$$X_b = [X_{b,1} \ X_{b,2} \ \dots \ X_{b,i} \ \dots \ X_{b,N_{be}+1}] ; N_{be} = \sum_{i=1}^{n_{span}} n_{be_i} \text{ with } :X_{b,i} = [y_{b,i} \ \theta_{zb,i}] \tag{19}$$

- The sub-matrix of the train is a diagonal matrix of order $10N_v \times 10N_v$ expressed as follows: $M_{vv} = \text{diag}(M_{v1} \ \dots \ M_{vj} \ \dots \ M_{vN_v})$ (20)

Where M_{vj} is the mass sub-matrix of order 10×10 of the $j - i\grave{e}me$ vehicle whose expression is :

$$M_{vj} = \text{diag}(m_c \ I_c \ m_b \ I_b \ m_b \ I_b \ m_w \ m_w \ m_w \ m_w) \quad (21)$$

With $\begin{cases} m_c: \text{masse d'une caisse de véhicule} \\ I_c: \text{module d'inertie d'une caisse} \\ m_b: \text{masse d'un bogie} \\ I_b: \text{module d'inertie d'un bogie} \\ m_w: \text{masse d'un essieu} \end{cases}$

- The rail mass sub-matrix is a diagonal matrix of order $2(N_{re} + 1)$ as there are 2-ddl per node, induced by the rail itself and by the axle wheels:

$$M_{rr} = M_{rr1} + M_{rr2} \quad (22)$$

$$M_{rr1} = \sum_{i=1}^{N_{re}} \int_0^{l_{re}} \overline{m_r} N_{ri}^T N_{ri} d\xi \quad (23)$$

N_{ri} ($i=1,2,\dots,N_{re}$) is the vector of shape functions for i -th rail element of order $1 \times 2(N_{re} + 1)$. To construct N_{ri} at each iteration, cancel all elements of the vector except the elements corresponding to the four ddl of the two nodes of the rail element: $N_{ri} = [0 \ 0 \ \dots \ N_{r,1} \ N_{r,2} \ N_{r,3} \ N_{r,4} \ \dots \ 0]$, where $N_{r,1}$ is at position $2i - 1$.

The ddl of the wheels are not independent, but linked to the ddl of the rail. This is why in the formulation of the global mass matrix we have M_{rr2} induced by all axle masses.

$$M_{rr2} = \sum_{j=1}^{N_v} \sum_{h=1}^{h=4} m_w N_{jh}^T N_{jh} \quad (25)$$

The size vector $1 \times 2(N_{re} + 1)$ $N_{jh} = [0 \ 0 \ \dots \ N_{r,1} \ N_{r,2} \ N_{r,3} \ N_{r,4} \ \dots \ 0]$ is evaluated at the local position ξ_{jh} ($h = \overline{1}$ which represents the distance between the h -th axle of the j vehicle and the left node of the rail element on which the axle acts. For N_{jh} ($h = \overline{4}$, apart from the elements corresponding to the four ddl of the two nodes of the rail element on which the vehiclewheels act, the other elements are zero.

In concrete terms, the positions of the axles of the vehicle of interest must be determined j then deduce their action rail $i(h)$ and their respective local coordinates at each instant t .

$$\begin{cases} x_{j1} = v_0 t + (j - 1)D_{vv} \\ x_{j2} = x_{j1} + 2l_b \\ x_{j3} = x_{j1} + 2l_c \\ x_{j4} = x_{j1} + 2(l_b + l_c) \end{cases}, \text{ où } D_{vv} \text{ est la distance entre deux véhicules consécutifs.} \quad (27)$$

Thus,

$$i(h) = Ent(x_{jh}/l_{re}) + 1; \xi_{jh} = [x_{jh} - Ent(x_{jh}/l_{re}) \times l_{re}] / l_{re} \quad (28)$$

Where $Ent()$ is the integer function.

- The sub-matrix of the sleepers is a square matrix of order $N_s \times N_s$,

$$M_{ss} = diag[m_s m_s \dots m_s] \quad (29)$$

- At the bridge, $M_{bb} = \sum_{i=1}^{N_{be}} \int_0^{l_{be}} \overline{m_b} N_{bi}^T N_{bi} d\xi \quad (30)$

In the same way as with the rail element, note that the vector N_{bi} ($i=1,2, \dots, N_{be}$) is the vector of shape functions for i -th bridge element of order $1 \times 2(N_{be} + 1)$. To construct N_{bi} at each iteration, cancel all elements of the vector except the elements corresponding to the four ddl of the two nodes of the rail element: $N_{bi} = [00 \dots N_{b,1} N_{b,2} N_{b,3} N_{b,4} \dots 0] \quad (31)$, where $N_{b,1}$ is at the position $2i - 1$.

- For the train, the global matrix is composed of the matrices of the elementary

vehicles:
$$K_{vv} = diag[K_{v1} \dots K_{vj} \dots K_{N_v}] \quad (32)$$

Where K_{vj} is the mass sub-matrix of order 10×10 of the j - ième vehicle whose expression is:

$$K_{vj} = \begin{bmatrix} 2k_s & 0 & 0 & 0 & 0 & 0 & 0 & 0 & 0 & 0 \\ 0 & 2k_s L_c^2 & 0 & 0 & 0 & 0 & 0 & 0 & 0 & 0 \\ -2k_p - k_s & 0 & 2k_p & 0 & 0 & 0 & 0 & 0 & 0 & 0 \\ 0 & 0 & 0 & 2k_p L_b^2 & 0 & 0 & 0 & 0 & 0 & 0 \\ -2k_p - k_s & 0 & 0 & 0 & 2k_p & 0 & 0 & 0 & 0 & 0 \\ 0 & 0 & 0 & 0 & 0 & 2k_p L_b^2 & 0 & 0 & 0 & 0 \\ 0 & 0 & -k_p & 0 & 0 & 0 & k_p & 0 & 0 & 0 \\ 0 & 0 & -k_p & 0 & 0 & 0 & 0 & k_p & 0 & 0 \\ 0 & 0 & 0 & 0 & -k_p & 0 & 0 & 0 & k_p & 0 \\ 0 & 0 & 0 & 0 & -k_p & 0 & 0 & 0 & 0 & k_p \end{bmatrix} \quad (33)$$

Identically we have :

$$C_{vj} = \begin{bmatrix} 2c_s & 0 & 0 & 0 & 0 & 0 & 0 & 0 & 0 & 0 \\ 0 & 2c_s L_c^2 & 0 & 0 & 0 & 0 & 0 & 0 & 0 & 0 \\ -2c_p - c_s & 0 & 2c_p & 0 & 0 & 0 & 0 & 0 & 0 & 0 \\ 0 & 0 & 0 & 2c_p L_b^2 & 0 & 0 & 0 & 0 & 0 & 0 \\ -2c_p - c_s & 0 & 0 & 0 & 2c_p & 0 & 0 & 0 & 0 & 0 \\ 0 & 0 & 0 & 0 & 0 & 2c_p L_b^2 & 0 & 0 & 0 & 0 \\ 0 & 0 & -c_p & 0 & 0 & 0 & c_p & 0 & 0 & 0 \\ 0 & 0 & -c_p & 0 & 0 & 0 & 0 & c_p & 0 & 0 \\ 0 & 0 & 0 & 0 & -c_p & 0 & 0 & 0 & c_p & 0 \\ 0 & 0 & 0 & 0 & -c_p & 0 & 0 & 0 & 0 & c_p \end{bmatrix} \quad (34)$$

- For the rail, K_{rr} is a sub-matrix of order $2(N_{re} + 1) \times 2(N_{re} + 1)$ defined by:

$$K_{rr} = K_{rr1} + K_{rr2} + K_{rr3} \quad (35)$$

$$K_{rr1} = \sum_{i=1}^{N_r} \int_0^{l_{re}} E_r I_r N_{ri}''^T N_{ri}'' d\xi, K_{rr2} = \sum_{j=1}^{N_v} \sum_{h=1}^4 k_p N_{jh}^T N_{jh}, K_{rr3} = \sum_{u=1}^{N_s} k_{rs} N_{r,u}^T N_{r,u} \quad (36)$$

The vectors of functions of forms $N_{jh} N''$ are the same as those defined in the previous paragraph. The prime exponent (") means the second derivative with respect to the local coordinate ξ . The vector of functions of form $N_{r,u}$ ($u = 1, \dots, N_s$) is evaluated at the relative position $\xi_{r,u}$ of the u -th tie (or crossbar). The shape function vector is evaluated at the relative position of the i -th tie (or crossbar).

$$x_u = (u - 1)l_{sp} \quad (37)$$

$$i(u) = 1 + Ent(x_u/l_{re}); \quad (38) \quad \xi_{r,u} = [x_u - Ent(x_u/l_{re}) \times l_{re}] / l_{re} \quad (39)$$

$$N_{r,u} = [0 \quad 0 \quad \dots \quad N_{r,1} \quad N_{r,2} \quad N_{r,3} \quad N_{r,4} \quad \dots \quad 0]_{\xi=\xi_{r,u}} \quad (40), N_{r,1} \text{ is at the position } 2i - 1.$$

The damping sub-matrix is similarly defined in terms of the matrices C_{rr2} of all vehicles and C_{rr3} of all attachments.

$$C_{rr2} = \sum_{j=1}^{N_v} \sum_{h=1}^4 c_p N_{jh}^T N_{jh} \quad (41), C_{rr3} = \sum_{u=1}^{N_s} c_{rs} N_{r,u}^T N_{r,u} \quad (42)$$

The sub-matrix of the sleepers is a square matrix of order $N_s \times N_s$,

$$K_{ss} = \text{diag}[k_{rs} + k_{sb}k_{rs} + k_{sb} \dots k_{rs} + k_{sb}] \quad (43)$$

$$C_{ss} = \text{diag}[c_{rs} + c_{sb}c_{rs} + c_{sb} \dots c_{rs} + c_{sb}] \quad (44)$$

The stiffness sub-matrix for the bridge is a square matrix of order $2(N_{be} + 1)$ composed of the stiffness matrix of the bridge itself and the stiffness matrix induced by the ballast:

$$K_{bb} = K_{bb1} + K_{bb2} \quad (45)$$

$$K_{bb1} = \sum_{i=1}^{N_{be}} \int_0^{l_{be}} E_b I_b N_{b,i}''^T N_{b,i}'' d\xi \quad (46), K_{bb2} = \sum_{g=1}^{N_s} k_{sb} N_{b,g}^T N_{b,g} \quad (47)$$

The vector $N_{b,i}$ ($i=1,2, \dots, N_{be}$) is defined in the previous paragraph as the vector of shape functions for an i -th bridge element. The vector of shape functions $N_{b,g}$ ($g = 1, \dots, N_s$) is evaluated at the relative position $\xi_{b,g}$ of the g -th ballast (or sleeper). To construct $N_{b,g}$ all elements of the vector except those corresponding to the four ddl of the two nodes of the bridge element containing this ballast must be cancelled. $x_g = (g - 1)l_{sp}$ Similarly, we construct the damping submatrix by summing the contributions of the on itself and the ballast: $C_{bb} = C_{bb1} + C_{bb2}$. For the first component, we will use the

Rayleigh formulation [Chopra A. K., 2011].

$$C_{bb_1} = a_0 M_{bb} + a_1 K_{bb_1} \quad (48)$$

$$a_0 = \xi \frac{2\omega_1\omega_2}{\omega_1 + \omega_2} \quad (49); \quad a_1 = \xi \frac{2}{\omega_1 + \omega_2} \quad (50)$$

Where ω_1, ω_2 are the first two modes of the bridge, and ξ its damping coefficient

$$C_{bb_2} = \sum_{g=1}^{N_s} c_{sb} N_{b,g}^T N_{b,g} \quad (51)$$

Vehicle-rail interaction sub-matrices

$$K_{vr} = \sum_{j=1}^{N_v} \sum_{h=1}^4 K_{jh} = \sum_{j=1}^{N_v} \sum_{h=1}^4 k_p N_{jh}^T N_{jh} \quad (52)$$

$$C_{vr} = \sum_{j=1}^{N_v} \sum_{h=1}^4 C_{jh} \quad (53)$$

$$K_{rv} = K_{vr}^T \quad (54)$$

Rail-sleeper interaction sub-matrices

K_{rs} is a matrix $2(N_{re} + 1) \times N_s$

$$K_{rs} = k_{rs} \begin{bmatrix} -N_{r,1}^T & -N_{r,2}^T & \dots & -N_{r,u}^T & \dots & -N_{r,N_s}^T \end{bmatrix} \quad (55)$$

$$C_{rs} = c_{rs} \begin{bmatrix} -N_{r,1}^T & -N_{r,2}^T & \dots & -N_{r,u}^T & \dots & -N_{r,N_s}^T \end{bmatrix} \quad (56)$$

The cross-bridge interaction sub-matrices:

$$K_{sb} = k_{sb} \begin{bmatrix} -N_{b,1}^T & -N_{b,2}^T & \dots & -N_{b,g}^T & \dots & -N_{b,N_s}^T \end{bmatrix}; \quad K_{bs} = K_{sb}^T \quad (58)$$

$$C_{sb} = c_{sb} \begin{bmatrix} -N_{b,1}^T & -N_{b,2}^T & \dots & -N_{b,g}^T & \dots & -N_{b,N_s}^T \end{bmatrix}; \quad C_{bs} = C_{sb}^T \quad (59)$$

In the coupling formalism we have used, the contact forces between the vehicle and the track will not necessarily be calculated because they are internal forces. Therefore, the vector of external forces will only include the self-weight and the dynamic excitation.

Force acting on the vehicle: The sub vector of forces acting on the train is the column vector F_v of order $10N_v$ of the forces exerted on each vehicle j noted F_{vj}

$$F_v = [F_{v_1} F_{v_2} \dots F_{v_{N_v}}]^T \tag{60}$$

$$F_{v_j} = F_{v_j}^1 + F_{v_j}^2, \tag{61}$$

Let us use the formulation of [Lou P. et al., 2012],

$$F_{v_j}^1 = \begin{bmatrix} 0 \\ 0 \\ k_p [2h(x_{j_1}^V) + 2h(x_{j_2}^V)] \\ k_p l_b [2h(x_{j_1}^V) - 2h(x_{j_2}^V)] \\ k_p [2h(x_{j_3}^V) + 2h(x_{j_4}^V)] \\ k_p l_b [2h(x_{j_3}^V) - 2h(x_{j_4}^V)] \\ \frac{W_{axle} \cdot \lambda}{b_0} h(x_{j_1}^A) \\ \frac{W_{axle} \cdot \lambda}{b_0} h(x_{j_2}^A) \\ \frac{W_{axle} \cdot \lambda}{b_0} h(x_{j_3}^A) \\ \frac{W_{axle} \cdot \lambda}{b_0} h(x_{j_4}^A) \end{bmatrix} \tag{62}$$

$$F_{v_j}^2 = \begin{bmatrix} 0 \\ 0 \\ c_p [2\dot{h}(x_{j_1}^V) + 2\dot{h}(x_{j_2}^V)] \\ c_p l_b [2\dot{h}(x_{j_1}^V) - 2\dot{h}(x_{j_2}^V)] \\ c_p [2\dot{h}(x_{j_3}^V) + 2\dot{h}(x_{j_4}^V)] \\ c_p l_b [2\dot{h}(x_{j_3}^V) - 2\dot{h}(x_{j_4}^V)] \\ f_{j_1}^{22} \left[\dot{h}(x_{j_1}^A) + \frac{1}{2} \dot{h}(x_{j_1}^G) \right] \\ f_{j_2}^{22} \left[\dot{h}(x_{j_2}^A) + \frac{1}{2} \dot{h}(x_{j_2}^G) \right] \\ f_{j_3}^{22} \left[\dot{h}(x_{j_3}^A) + \frac{1}{2} \dot{h}(x_{j_3}^G) \right] \\ f_{j_4}^{22} \left[\dot{h}(x_{j_4}^A) + \frac{1}{2} \dot{h}(x_{j_4}^G) \right] \end{bmatrix} \tag{63}$$

With h is the generating function of the random spatial variation of irregularities, \dot{h} its first derivative with respect to time, W_{axle} the maximum axial load of a vehicle, λ a parameter characterising the inclination of the rail as a function of the rail-to-wheel contact point.

$$\dot{h}() = \lim_{\Delta t \rightarrow 0} \frac{\Delta h}{\Delta t} = \lim_{\Delta t \rightarrow 0} \frac{\Delta h}{\Delta x/v_0} = v_0 \cdot \lim_{\Delta t \rightarrow 0} \frac{\Delta h}{\Delta x} = v_0 \cdot \frac{\partial h}{\partial x} \quad (64)$$

$$\dot{h}(x) = -v_0 \cdot \sum_k (\sqrt{2k^2 \Delta F^3 S_{zz,k}(k\Delta F)} \sin(k\Delta Fx + \varphi_k)) \quad (65)$$

The exponents on x^V , x^A , x^G respectively represent the abscissa x of the levelling, alignment, and track gauge irregularities at the position of the h -th wheel of the vehicle j .

The term f^{22} represents the transverse pseudo-slip coefficient between the rail and the j -th wheel of the j -th vehicle.

The force on the rail F_r is the order matrix $N_{re} \times 1$ which is calculated for the points on the rail concerned by:

$$F_r = F_0 + F_V + F_A + F_3 + F_4 + F_5 + F_6 \quad (66)$$

F^0 Force vector of the loads on each axle due to the weight on the rail

F^1 Force vector of the loads on each axle due to rail levelling irregularities

F^2 Force vector of the loads on each axle due to rail alignment irregularities

F^3 Vector force of the loads on each axle due to irregularities and track gauge

F^4 Force vector of the loads on each axle due to the derivative of the rail levelling irregularities

F^5 Force vector of the loads on each axle due to the derivative of the rail alignment irregularities

F^6 Force vector of the loads on each axle due to the derivative of the irregularities and the track gauge

All elements in the sub-vectors of the forces on the crossbeams F_s order $N_s \times 1$ and on the F_b order bridge $2(N_{be} + 1) \times 1$ is zero. Practical simulation: the case of the second bridge over the Wouri

Data and working assumptions for the case study

Table 1: Train parameters used for the simulation.

Rating	Description	Value	Unit
m_c	Weight of the box	4.175×10^4	Kg
I_c	Modulus of inertia of the body	2.08×10^6	Kg.m ²
l_c	Half axle between bogies	6.0	m
l_b	Half axle distance between bogie axles	1.25	m
k_p	Primary suspension spring rate	1.18×10^6	N/m
c_p	Primary suspension damping	3.92×10^4	N s/m

k_s	Secondary suspension stiffness	5.3×10^5	N/m
c_s	Secondary suspension damping	9.02×10^4	N s/m
m_b	Mass of a bogie	3.04×10^3	Kg
I_b	Module of inertia of a bogie	3.93×10^3	Kg.m ²
m_w	Mass of an axle	1.78×10^3	Kg
v	Locomotive speed	$60 \leq v \leq 220$	km/h

The bridge is a successive cantilever bridge consisting of eight beams $23+91+129.5 \times 4+91+23=746$ m.

Table 2: Table of track parameters.

Rating	Description	Value	Unit
The bridge			
A_b	Cross-section	12.83	m ²
E_b	Young's modulus	40.52×10^6	N/m ²
I_{be}	Inertia module	3.81	m ⁴
m_{be}	Mass per unit length	3.4188×10^4	Kg/m
ξ_b	Depreciation coefficient	1	%
l_{be}	Length of the bridge element	5.16	m
The rail			
A_r	Cross-section	77.45×10^{-4}	m ²
Rating	Description	Value	Unit
E_r	Young's modulus	210×10^9	N/m ²
I_r	Inertia module	3.22×10^{-5}	m ⁴
D_{rroue}	Half distance between rail centres	0.50	m
m_r	Mass per unit length	60.64	Kg/m
$l_{\mathfrak{R}}$	Length of the rail element	0.645	m
Fasteners and ballast			
k_{rs}	Stiffness of fasteners	6.0×10^7	N/m
c_{rs}	Fastener damper	7.5×10^4	N s/m
k_{sb}	Ballast stiffness	2.25×10^8	N/m
c_{sb}	Ballast damper	6.0×10^4	N s/m
Crossings			
m_s	Mass of the crossbar	680	Kg
l_{sp}	Crossbar spacing	0.645	m

We make some simplifying assumptions to implement the methodology.

1. We consider an isolated locomotive, i.e. $N_v = 1$.
2. The bridge is We assume that the beams are of equal length, $129 \times 6 = 774$ m.
3. The finite elements adopted for this work are such that $:n(l_{re}; l_{be}) = (0,645 ; 5,16) [m] \leftrightarrow (N_{re}; N_{be}) = (1200 ; 150)$
4. The ballast and ties are discretized under sleepers spaced at $l_{sp} = l_{re} = 0,645$ m which is a

sufficiently fine mesh.

5. The rail surfaces are assumed to be smooth in the first instance, and in good condition in the second instance (with simulation of irregularities with the German PSD generator function). The irregularities taken into account are alignment (S^V) and longitudinal (S^A).
6. The additional effect of the displacements of the bridge structure on the irregularity is neglected.

1.3 RESULTS AND DISCUSSION

The equation is of the form

$$\begin{bmatrix} M_{vv} & 0 & 0 & 0 \\ 0 & M_{rr} & 0 & 0 \\ 0 & 0 & M_{ss} & 0 \\ 0 & 0 & 0 & M_{bb} \end{bmatrix} \begin{Bmatrix} \ddot{X}_v \\ \ddot{X}_r \\ \ddot{X}_s \\ \ddot{X}_b \end{Bmatrix} + \begin{bmatrix} C_{vv} & C_{vr} & 0 & 0 \\ C_{rv} & C_{rr} & C_{rs} & 0 \\ 0 & C_{sr} & C_{ss} & C_{sb} \\ 0 & 0 & C_{bs} & C_{bb} \end{bmatrix} \begin{Bmatrix} \dot{X}_v \\ \dot{X}_r \\ \dot{X}_s \\ \dot{X}_b \end{Bmatrix} + \begin{bmatrix} K_{vv} & K_{vr} & 0 & 0 \\ K_{rv} & K_{rr} & K_{rs} & 0 \\ 0 & K_{sr} & K_{ss} & K_{sb} \\ 0 & 0 & K_{bs} & K_{bb} \end{bmatrix} \begin{Bmatrix} X_v \\ X_r \\ X_s \\ X_b \end{Bmatrix} = \begin{Bmatrix} F_v \\ F_r \\ F_s \\ F_b \end{Bmatrix}$$

Where M, C and K denote the mass, damping and elasticity sub-matrices respectively, X and F represent the displacement and force vectors respectively, and the subscripts "v", "r", "s" and "b" denote the vehicle, rail, sleeper and bridge, respectively

$$\begin{aligned} X_v &= [y_c \ \theta_{zc} \ y_{b1} \ \theta_{zb1} \ y_{b2} \ \theta_{zb2} \ y_{w1} \ y_{w2} \ y_{w3} \ y_{w4}]^T \\ X_r &= [X_{r,1} \ X_{r,2} \ \dots \ X_{r,i} \ \dots \ X_{r,1201}]^T \text{ with : } X_{r,i} = [y_{r,i} \ \theta_{zr,i}]^T \\ X_s &= [y_{s1} \ y_{s2} \ \dots \ y_{sN_s}]^T \\ X_b &= [X_{b,1} \ X_{b,2} \ \dots \ X_{b,i} \ \dots \ X_{b,151}]^T \text{ with : } X_{b,i} = [y_{b,i} \ \theta_{zb,i}]^T \end{aligned}$$

When the rail surface is assumed to be rough, the German PSD generator function can simulate the random irregularities in the vertical plane shown in figure 7.

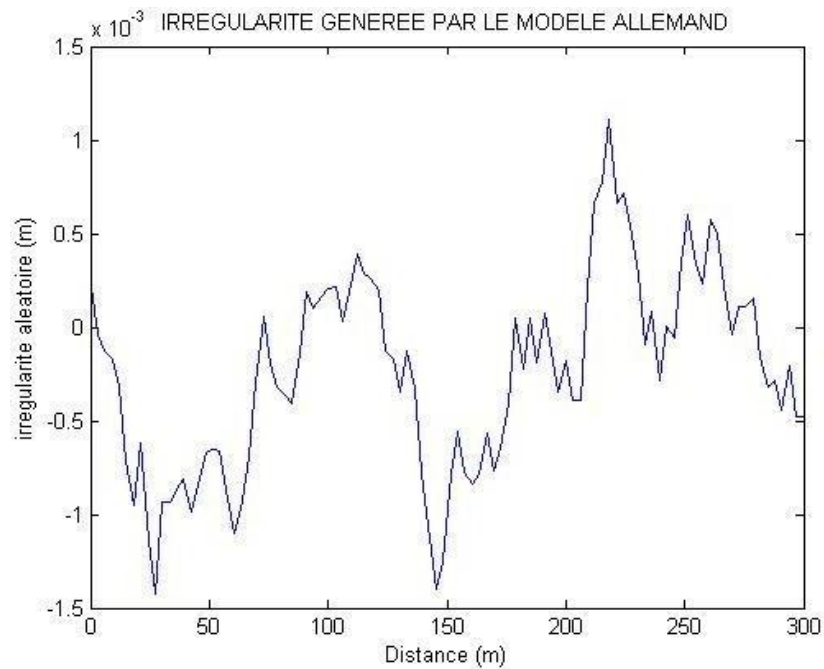


Figure 7: Track irregularities transformed by the German spectrum.

The resolution of the dynamic interaction system gives the temporal evolution of the system response in terms of displacements $X(t)$, velocities $\dot{X}(t)$ and accelerations $\ddot{X}(t)$ at all nodes of the system under study. From this, the magnitude of this response can be appreciated as a function of the vehicle speed, the type of train loading and the track condition.

$$\begin{aligned}\omega_0 &= 1,0075 \times 10^{14} \text{ rad/s} && \text{max} \\ \omega_0 &= 3,070 \times 10^3 \text{ rad/s} && \text{min}\end{aligned}$$

The track response is speed dependent, e.g. maximum vertical rail displacement of 0.0942m or approx. $v_{max} = 220(\text{km/h})$. For example, the maximum vertical displacement of the rails is 0.0942m or about 94mm; the maximum displacement of the bridge is 0.153m or about 153mm (figure 8 below).

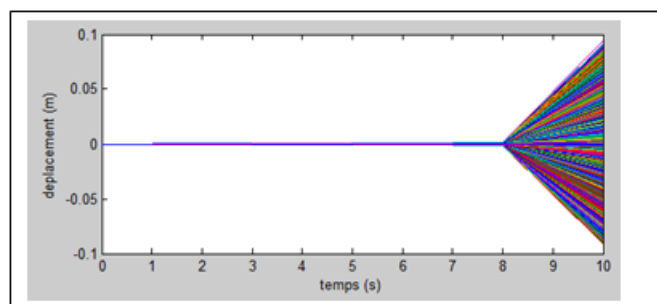


Figure 8: Time diagrams of rail node displacements and accelerations at 220km/h.

There are twice as many nodes on the rail element as on the bridge element, hence the diagram is denser above than below (it's illustrated in figure 9).

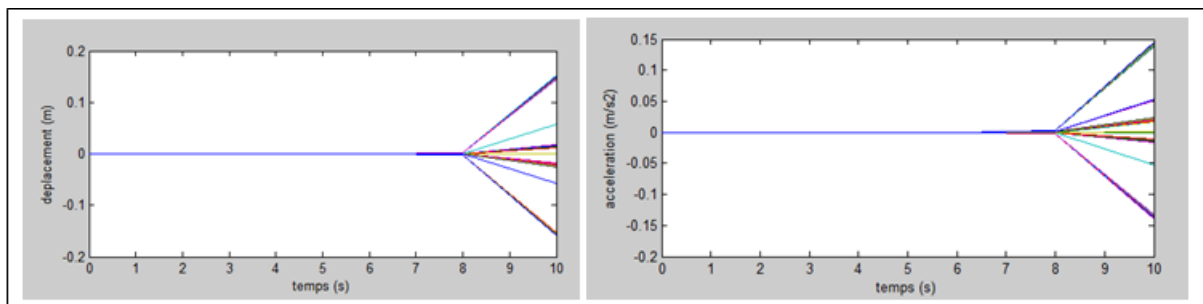


Figure 9: Time diagram of bridge node displacements and accelerations at 220km/h

Knowing that the deflection is limited to $L/500=258\text{mm}$, it can be seen that the condition for limiting the deflection is verified. But we can notice a limit of the model when the train is not completely on the bridge.

In figure 10, 11 we show the results for the low speed 60 km/h.

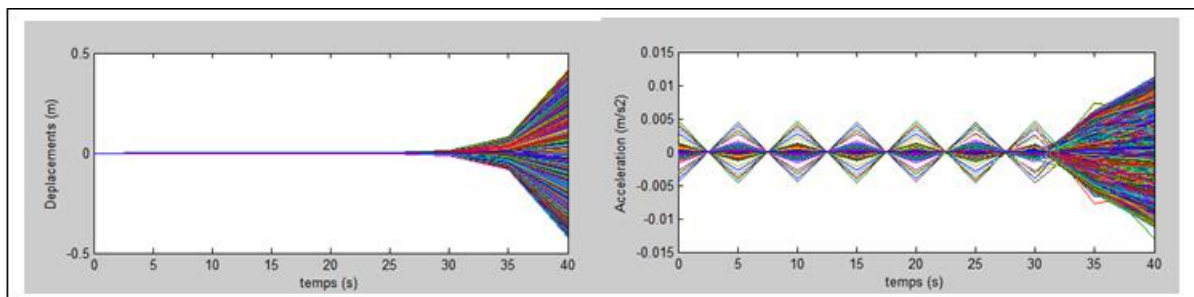


Figure 10: Time diagram of rail node displacements and accelerations at 60km/h

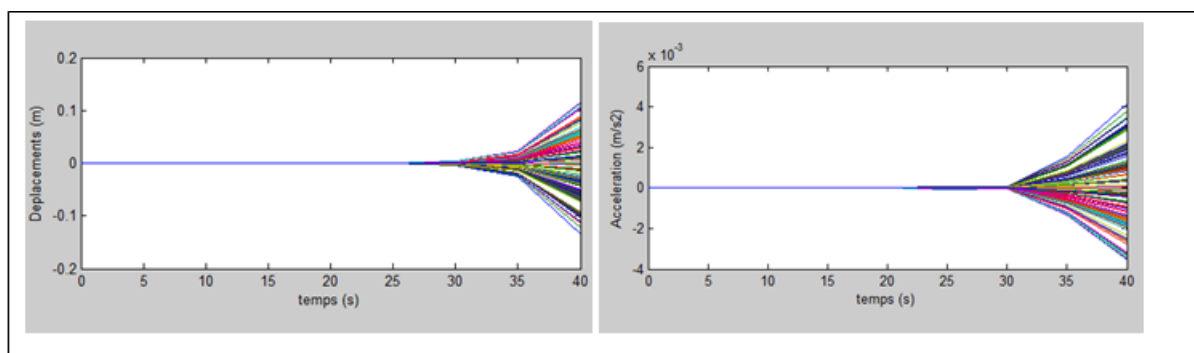


Figure 11: Time diagrams of displacements and accelerations of bridge nodes at 60km/h

We test the model with other velocity values in order to draw a graph about simulation of maximum bridge displacements as a function of speed (figure 12).

$Av = 150(km/h)$ maximum rail displacement is 32mm; maximum bridge displacement is 52mm.

$Av = 100(km/h)$ maximum rail displacement of 19mm; maximum bridge displacement of 5mm.

$Av_{min} = 60(km/h)$ The result is a small rail displacement of 14mm; a maximum bridge displacement of 3.8mm.

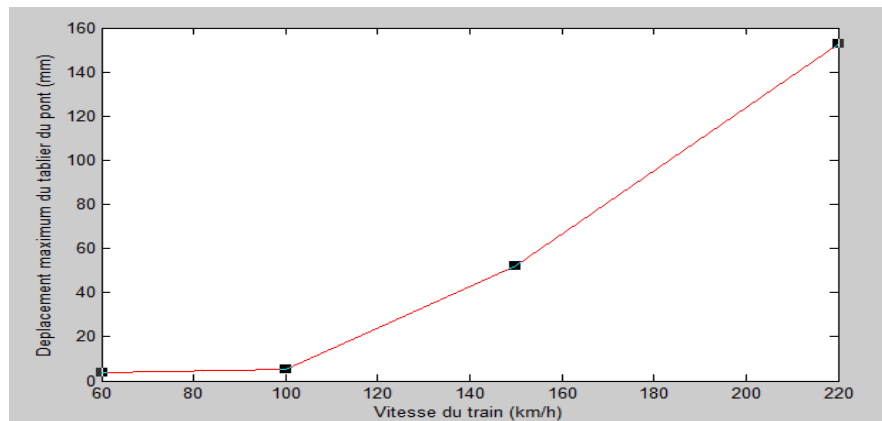


Figure 12: Simulation of maximum bridge displacements as a function of speed.

These results make it possible to deduce the dynamic forces on the bridge knowing its structural characteristics up to the foundation. It can also be noted that the bridge does not enter into resonance up to 220 km/h. The trend of the results suggests that the structure of the 2nd bridge over the Wouri could support modern fast locomotives. The model of this paper is satisfying despite the fact that we note a limit of the model when the train is not completely on the bridge.

2. General conclusion and outlook

The work we have carried out in this paper aimed at allowing a quick calculation of the dynamic responses of the railways in order to facilitate the selection of the existing rail bridges suitable to receive a modernised railway fleet. The main excitation of the system is the set of geometrical defects of the track, modelled by the sinusoidal function PSD of the German model because it is the most complete model in defect typology. Through FEM, we worked with a three-layer track model with unequal elements and a vehicle model with 10 degrees of freedom. For the case study on the second bridge over the Wouri, a system of equations with 3914 unknowns (vertical displacements and rotations) was obtained and solved by the iterative method. The dynamic displacements and accelerations of the rails and the bridge at each node were calculated when a locomotive passes. It was found that this bridge would be

able to accommodate locomotives at higher speeds (220km/h) as the displacements remain below 258mm (the maximum being 90mm) and the accelerations. The fact that the bridge has a large curved section leaves some doubt as to the limitation of centrifugal acceleration which will need to be investigated. Our work could be extended to the calculation of the centrifugal acceleration, making it more relevant in 3D, i.e. taking into account the transverse parameters of the structure, its lateral behaviour. It would also be necessary to take into account the behaviour of the rails and the bridge when the train is not entirely on the bridge and when it involves the continuity of the railway track, which rests on natural or stabilised soil whose mechanical and structural properties are extremely different from the bridge structure. Through an in-depth investigation, it would be interesting to multiply the case studies to all the railway bridges of Cameroon in order to recognize the most suitable for modernity.

BIBLIOGRAPHIC REFERENCES

1. AFNOR European Standard EN 1992-1-1. - Eurocode 2: Design of concrete structures - Part 2: Actions on bridges due to traffic, 2004.
2. AFNOR European Standard EN 1990/A1. Eurocode 0: Basis for structural design - Amendment A1, 2008.
3. African Development Bank Rail Infrastructure in Africa - Financing Policy Options, 2015; 207.
4. Cantero Daniel, Arvidsson Therese, Obrien Eugene, Karoumi Raid Train-track-bridge modelling and review of parameters. Structure and Infrastructure Engineering, 2015; 29.
5. Chopra Anil K. Dynamics of Structures: Theory and Applications to Earthquake Engineering, 4th Ed. Prentice Hall, USA, 2011; 945.
6. Cui Y.-J., Lamas-Lopez F., Trinh V. N., Calon N., Costa D'Aguiar S., Dupla J.-C., Tang A. M., Canou J. and Robinet A. Investigation of interlayer soil behaviour by field monitoring. Transportation Geotechnics, 2014; 1(3): 91-105.
7. Esveld C. Modern Railway Track, Second Edition. MRT-Productions, Zaltbommel, 2001.
8. Khaled E. Zaazaa and A. L. Schwab Review of Joost Kalker's Wheel-Rail Contact Theories And Their Implementation In Multibody CODES. Proceedings of the ASME International Design Engineering Technical Conferences & Computers and Information in Engineering Conference. IDETC/CIE 2009 August 30 - September 2, San Diego, California, USA., 2009.
9. Kourousis Georges Modelling the vibratory effects of railway traffic on the environment. PhD in Engineering Sciences, Faculté Polytechnique de Mons, Belgium, 2009.

10. Kouroussis G., Connolly D.P. and Verlinden O. Railway-induced ground vibrations - a review of vehicle effects, *International Journal of Rail Transportation*, 2014; 2(2): 69-110. DOI: 10.1080/23248378.2014.897791.
11. Leboeuf Michel High-Speed Rail: Opportunities and Threats. *Engineering*, 2016; 2: 402-408.
12. Lou Ping, Yu Zhi-Wu, F.T.K. A Rail-bridge coupling element of unequal lengths for analyzing train-track-bridge interaction systems. *Applied Mathematical Modelling*, 2012; 36(4): 1395-1414.
13. Olievski V. N. Rail transport. An analytical framework for improving rail performance, in sub-Saharan Africa. SSAP, Working Paper, 2013; 94: 95.
14. Pourtier Roland Les chemins de fer en Afrique subsaharienne, entre passé révolu et recompositions incertaine, *Belgeo*, 2007; 2: 189-202.
15. Quezada Juan Carlos Ballast settlement mechanisms and its variability. PhD thesis in Mechanics and Civil Engineering, Department of Geotechnics. Université Montpellier II - Sciences et Techniques du Languedoc, 2012; 159.
16. SNCF Référentiel Technique pour la réalisation des LGV - Partie Génie Civil. Référentiel Infrastructure IN, 2006; 3278.
17. Toumi Moncef Numerical modelling of the wheel-rail contact for the study of the parameters influencing the Kalker coefficients: Application to railway dynamics. PhD thesis in Mechanics, Department of Materials. Université Paris-Est, 2016; 181.
18. Zeng Zhi-Ping, Liu Fu-Shan, Lu Zhao-Hui, Yu Zhi-Wu, Lou Ping and Chen Ling-Kun. Three-Dimensional Rail-Bridge Coupling Element of Unequal Lengths for Analyzing Train-Track-Bridge Interaction System. *Latin American Journal of Solids and Structures*, 2016; 13: 2490-2528.
19. Zhang Nan, He Xia, Weiwei Guo, Jiawang Zhan, Jinbao Yaou, Yanmei Cao Vehicle-bridge interaction analysis of heavy load railway. *Procedia Engineering*, 2010; 4: 347-354.
20. Zhang Nan, Yuan Tian, He Xia A train-bridge dynamic interaction analysis method and its experimental validation. *Engineering*, 2016; 2: 528-536.